International Journal of Knowledge Discovery in Bioinformatics
Volume 6 • Issue 2 • July-December 2016

Predictive Toxicity of Conventional Triazole Pesticides by Simulating Inhibitory Effect on Human Aromatase CYP19 Enzyme

Tamar Chachibaia, University of Santiago de Compostela, Santiago de Compostela, Spain and Tbilisi State University, Tbilisi, Georgia

Joy Harris Hoskeri, Institute of Experimental Toxicology and Pharmacology, Bratislava, Slovakia

ABSTRACT

15 common fungicides were evaluated to study their inhibitory effects on the human aromatase enzyme in comparison with the Letrozole (LTZ), the most potent inhibitor of aromatase (AI) used as anti-estrogen for breast cancer treatment using AUTODOCK software for calculation of inhibition energy on CYP19A1 aromatase enzyme. Those compounds with minimal binding energy are safer in terms of toxicity and resistance of other prescription drugs like non-steroid AIs. In the authors' study, they found that four triazole fungicides compounds, Triticonazole, Tebuconazole, Metconazole and Fluquinconazole, exhibited minimal inhibition constant (IC).

KEYWORDS

Aromatase Inhibitors, CYP19 Enzyme, In Silico, Pesticide, Risk Assessment, Triazoles

INTRODUCTION

Biosynthesis of estrogens from androgens is catalyzed by cytochrome P450 aromatase. Aromatase inhibition by the triazole compounds Letrozole (LTZ) and Anastrozole is a prevalent therapy for estrogen-dependent postmenopausal breast cancer.

Triazole fungicides are widely used as agricultural fungicides and antimycotic drugs that target 14α-demethylase. Some were previously shown to inhibit aromatase, thereby raising the possibility of endocrine disruptive effects. However, mechanistic analysis of their inhibition has never been undertaken.

We have evaluated the inhibitory effects of 15 common fungicides in human aromatase enzyme in comparison with the Letrozole (LTZ), the most potent inhibitor of aromatase used as anti-estrogen for breast cancer treatment using AUTODOCK software for calculation of inhibition energy on CYP19 aromatase enzyme (Egbuta, Lo, & Ghosh, 2014).

Triazole containing compounds as systemic fungicides are widely used in agriculture due to its high efficiency, broad spectrum, low toxicity and long effectiveness (Feng, Guo, Song, Hu, & Li, 2011). Currently 16 triazole fungicides: bitertanol, cyproconazole, difenoconazole, epoxiconazole, fluquinconazole, flusilazole, flutriafol, hexaconazole, metconazole, myclobutanil, penconazole, propiconazole, tebuconazole, triadimefon, triadimenol and triticonazole, are approved by Swiss Federal Office of Public Health (Zürich, Switzerland). Switzerland no longer allows the use of many chemicals that are still sprayed on American fields (Rosensteil, 2015). By 2005 was set the goal to halve the pesticide pollution of water bodies (Singer, 2002). Although, by 2014 report was released

DOI: 10.4018/IJKDB.2016070104

that in the five rivers in Switzerland's found heavily polluted in spring and summer by a cocktail of different pesticides (swissinfo.ch, 2014).

Target enzymes of triazoles in steroidogenesis are the sterol *14-alfa-demethylase* (encoded by the CYP51 gene) and the *aromatase* (encoded by the CYP19 gene).

The human aromatase enzyme is a member of the cytochrome P450 family and is the product of the *CYP19A1* gene, located on chromosome 15 (Thompson & Siiteri, 1974; Chen et al., 1988). Aromatase is the only known vertebrate enzyme that can aromatize a six-membered ring; aromatase is, therefore, the sole source of estrogen in the body (Amarneh, Corbin, Peterson, Simpson, & Graham-Lorence, 1993).

Nevertheless, since aromatase was first characterized, research has been impeded by the lack of its three-dimensional structure. In 2009, Ghosh *et al.* successfully solved the crystallized structure of human aromatase enzyme and provides a structural basis for the specificity to androgen (Ghosh, Griswold, Erman, & Pangborn, 2009; Ghosh, Griswald, Erman, & Pangborn, 2010).

The catalytic site of aromatase is located at the juncture of the I and F helices, β-sheet 3, and as the B-C loop. Androstenedione binds into the steroid binding pocket such that its β-face orientates towards the heme group of aromatase, placing C19 within 4.0 Å of the Fe atom. This binding site is only possible if the I-helix backbone is moved 3.5 Å, creating a binding pocket that is approximately 400 $Å^3$. This important distortion is created by residue P308, without which N309, steric hindrance would prevent catalytic activity.

This crystal structure of aromatase will not only allow better structure-based drug design than previous models, but it has also allowed a direct analysis of why some currently available aromatase inhibitors function better than others (Chumsri, Howes, Bao et al., 2011).

As triazole moieties are widely used in fungicides, some studies reported that agricultural triazole pesticides are culprits for the development of resistance to other triazole containing drugs (Snelders et al., 2012) e.g. triazole aromatase inhibitor antiestrogens. Among them are Anastrozole and Letrozole, the third-generation nonsteroidal aromatase inhibitors (AIs), which are now used as first-line therapy in the treatment of breast cancer in postmenopausal women (Scheme 2) (Brodie, 2002; Geisler, 2011; Brueggemeier, Hackett, & Diaz-Cruz, 2005). In recent years, some triazole residues have been found in agricultural products, including fruits, wheat, tea leaves and wine and water (Kumar, Ravindranath, & Shanker, 2004; Trosken, Bittner, & Volkel, 2005; Zhou, Xiao, & Ding, 2007; Jeannot, Sabik, Sauvard, & Genin, 2000; Paraiba, 2007). In one study was concluded that many azole compounds developed as inhibitors of fungal sterol 14-alfa-demethylase are inhibitors also of mammalian sterol 14-alfa-demethylase and mammalian aromatase with unknown potencies (Zarn, Bruschweiler, & Schlater, 2003).

To avoid the risk of possible development of resistance to other triazole drugs and to reduce toxicity of aromatase inhibitors in the treatment of breast cancer, there are used different methods in order to find out new preventive strategies.

In our study, we perform virtual screening of 15 fungicides and AI reference drug Letrozole to measure inhibitory effect on human aromatase. In this way, we aim to range which pesticides are most potent inhibitors of Cyp19 enzyme to predict and prevent possible summative cumulating effect of fungicide undesirably overlapping with the activity of anticancer drugs.

The publication of a high-resolution X-ray structure of human aromatase has opened the way to a greater understanding of the structural basis for estrogen synthesis and substrate/inhibitor recognition (Schuster et al., 2006). Triazole aromatase inhibitors (AIs) bind to the active site of CYP19 by coordinating the heme iron atom of the enzyme through a heterocyclic nitrogen lone pair.

In our docking study, we used together the X-ray structure of human cytochrome P450 aromatase Cyp19A1 (PDB code 3S79, resolution 2.75 Å) (Ghosh et al., 2012) associated with the metabolism of

Table 1. Results of docking of 15 fungicides and one non-steroid Aromatase inhibitor (NSAI) Letrosole

SL. NO.	MOLECULE	ORIENTATION	BINDING ENERGY Kcal/mole	DOCKING ENERGY Kcal/mole	INHIBITATION CONSTANT (Ki) (nM)	INTERMOL ENERGY	TORSIONAL ENERGY	INTERNAL ENERGY	RMSD	HYDROGEN BOND
1.	Bitertanol	7th	-6.19	-5.09	2.9 e-005	-8.06	1.87	2.97	0.0	2 H-BONDS WITH **ASP371, LEU372**
2.	Cyproconazole	10th	-9.25	-8.73	1.66 e-007	-10.81	1.56	2.08	0.0	1 H-BOND WITH **MET374**
3.	Difenoconazole	7th	-7.26	-6.83	4.03 e-006	-8.92	1.56	2.09	0.0	1 H-BOND WITH **THR310**
4.	Epoxiconazole	8th	-10.83	-12.58	1.04 e-008	-12.14	1.25	-0.44	0.0	1 H-BOND WITH **MET374**
5.	**Fluquinconazole**	9th	-17.25	-17.83	**2.29 e-013**	-17.87	0.62	0.04	0.0	
6.	Flutriafol	2nd	-8.7	-7.94	4.18 e-007	-9.95	1.25	2.01	0.0	
7.	Hexaconazole	7th	-10.72	-11.52	1.38 e-008	-12.59	1.87	1.07	0.0	1 H-BOND WITH **MET374**
8.	**Metconazole**	5th	-19.69	-19.92	**3.68 e-015**	-20.95	1.25	1.01	0.0	
9.	Myclobutanil	1st	-8.5	-8.1	5.92 e-007	-10.36	1.87	2.27	0.0	1 H-BOND WITH THR310
10.	Penconazole	6th	-7.71	-9.07	2.22 e-006	-9.27	1.56	0.2	0.0	1 H-BOND WITH THR310
11.	Propiconazole	3rd	-8.64	-10.17	4.64 e-007	-10.2	1.56	0.03	0.0	
12.	**Tebuconazole**	7th	-21.09	-21.91	**3.5 e-016**	-22.95	1.87	1.04	0.0	
13.	Triadimefon	4th	-8.46	-9.97	6.29 e-007	-10.02	1.56	0.04	0.0	
14.	Triadimenol	9th	-10.59	-11.37	1.72 e-008	-12.15	1.56	0.78	0.0	
15.	**Triticonazole**	2nd	-21.65	-21.96	**1.35 e-016**	-22.89	1.25	0.94	0.0	
16	**Letrozole**	7th	-9.54	-8.77	**1.01 e-007**	-10.48	0.93	1.71	0.0	

estrogens and carcinogens with breast cancer, with a collection of commercially available compounds, particularly, 15 triazole fungicides and anticancer drug Letrozole as reference standard (Table 1).

Molecular docking is established method for analysis of molecular associations, which is mostly used in the drug discovery field to study the binding of small molecules (ligands) to macromolecules (receptor) (Barril & Morley, 2005).

Cytochrome P450 aromatase homology models were published and used to perform docking and molecular dynamics simulations on known AIs (Favia, Cavalli, Masetti et al., 2006; Karkola, Holtje, & Wahala, 2007).

MATERIALS AND METHODS

The availability of X-ray structure of human aromatase enables us to set up docking protocol by AutoDock software to identify iron - ligand interactions between heme protein and 16 different triazole ligands, as chemical scaffolds able to inhibit aromatase, thus testing interactions within the aromatase binding site.

Computational ligand docking methodology, AutoDock 4.0, based on Lamarckian genetic algorithm (Solis & Wets, 1981) was employed for virtual screening of a compound library with 16 entries including reference compound as Letrozole, the 3rd generation aromatase inhibitors for the treatment of breast cancer, with the enzyme Cytochrome P450 aromatase(Cyp19A1), a potential drug target.

Autodock 4.0 uses GA as a global optimizer combined with energy minimization as a local search method (Morris et al., 1998).

The macromolecule, Cytochrome P450 aromatase or Cyp19A1 (PDB code 3S79, resolution 2.75 Å) was retrieved by using AutoDock 4 (The Scripps Research Institute, Molecular Graphics Laboratory, 10550 North Torrey Pines Road, CA, 92037) running on operative system Windows 7 (Miscosoft corporation 2007)

PRODRG was used to draw the 2D structures of different ligands. All the structures were written in protein database (PDB) format. Input molecules files for an AutoDock experiments must confirm to the set of atom types supported by it. Therefore, PDBQT format was used to write ligands, recognized by AutoDock.

Torsional degree of freedom (TORSDOF) is used in calculating the change in the free energy caused by the loss of torsional degree of freedom upon binding. In the AutoDock 4.0 force field, the TORSDOF value for a ligand is the total number of rotatable bonds in the ligand.

The 3D crystal structure of Cytochrome P450-aromatase Cyp19A1 (Figure 2) PDB code 3S79, resolution 2.75 Å was downloaded from Brookhaven Research Collaboratory for Structural Bioinformatics (RCSB) Protein Data Bank (PDB; http://www.rcsb.org/pdb).

The nonbonded oxygen atoms of waters, present in the crystal structure were removed. After assigning the bond orders, missing hydrogen atoms were added, then the partial atomic charges was calculated using Gasteiger–Marsili method (Gasteiger). United atom charges were assigned, non-polar hydrogens were merged, and rotatable bonds were assigned, considering all the amide bonds as non-rotatable. The receptor file was converted to PDBQT format, which is PDB plus ''q'' charges and ''t'' AutoDock type. (To confirm the AutoDock types, polar hydrogens should be present, whereas non-polar hydrogens and lone pair should be merged, each atom should be assigned Gasteiger partial charges). Amino acids which form target pocket or inhibition cite of aromatase

MOLECULAR DOCKING STUDY

In the present work, we have studied the in silico binding affinities to the active pocket (Figure 3) of enzyme 3S79 (Figure 2) to the selected 15 triazole fungicides (Figure 1) and the standard anti-aromatase drug Letrozole.

Of the three different search algorithms offered by AutoDock 4.0, the Lamarckian Genetic algorithm (LGA) based on the optimization algorithm was used in favor to other two - simulated annealing and genetic algorithm.

For all dockings, 10 independent runs with step sizes of 0.2Å for translations and 5Å for orientations and torsions were used. AutoDock tools along with AutoDock 4.0 and AutoGrid 4.0 was used to generate both grid and docking parameter files (i.e., gpf and.dpf files) respectively.

A grid box size of 42 x 42 x 42 Å points with a grid spacing of 0.375 Å was generated using AutoGrid (Morris et al., 1998). The grid was centered at x,y,z coordinates of 85.51, 52.282, 48.114, which was reported as the binding site residues.

For each docking experiment, the lowest energy docked conformation was selected from 10 runs. The successful completion of docking experiment took from 1 to 4 hours, on a 2.0 GHz Intel (R) core 2 duo machine with 3.0 GB of RAM and Windows 7 operating system.

Prior to actual docking run, AutoGrid 4.0 was introduced to precalculate grid maps of interaction energies of various atom types.

The energy of interaction of this single atom with the protein is assigned to the grid point. An affinity grid is calculated for each type of atoms in the substrate, typically carbon, oxygen, nitrogen, and hydrogens as well as grid of electrostatic potential using a point charge of 1 as the probe. Autodock 4.0 uses these interaction maps to generate ensemble of low energy conformations. It uses a scoring function based on AMBER force field, and estimates the free energy of binding of a ligand to its target. For each ligand atom types, the interaction energy between the ligand atom and the receptor is calculated for the entire binding site which is discretized through a grid. This has the advantage that interaction energies do not have to be calculated at each step of the docking process but only looked up in the respective grid maps.

Since a grid map represents the interaction energy as a function of the coordinates, their visual inspection may reveal the potential unsaturated hydrogen acceptors or donors or unfavorable overlaps between the ligand and the receptor.

RESULTS

The binding affinity was evaluated by the binding energies, docking energy, inhibition constant, intermolecular energy, and RMSD values. It was demonstrated that the docking protocol could reliably reproduce the interaction of aromatase with its substrate with an RMSD of 0 Å.

The results of LGA docking experiments of the triazoles using AutoDock 4.0 and AutoGrid 4.0 are summarized in Table 1.

Binding energy for reference compound Letrozole (Figure 7) in our docking study is comply with other studies and is in agreement with them (Suvannang, Nantasenamat, Isarankura-Na-Ayudhya et al., 2011).

Triazole compounds (Figures 4, 5, 6) 1, 3, 10 are chosen as possessing aromatase inhibitory potency based on obtained algorithmic parameters docking: highest binding energy, highest inhibition constant, and hydrogen bonds.

Compound 1 (Bitertanol) exhibits RMS equivalent to zero in 7th orientation to heme molecule of protein, and at this position binding energy is - 6,19; IC – 2,9X10-5; and two hydrogen bonds with amino acids of target pocket ASP371 and LEU372.

Compound 3 (Difenoconazole) demonstrated best compliance of inhibitory bound in 7th orientation to RMS=0 posing heme molecule, binding energy -7,36, IC – 4,03X10-6, and one hydrogen bond with target pocket amino acid THR310.

Compound 10 (Penconazole) exhibits its highest binding energy -7.71 at orientation 6th to heme molecule parallel alignment at RMS zero point, IC – 2.22X10-6 and one H-BOND with THR310.

Figure 1. Scheme 1. Downloaded from free public domain http://www.alanwood.net/pesticides

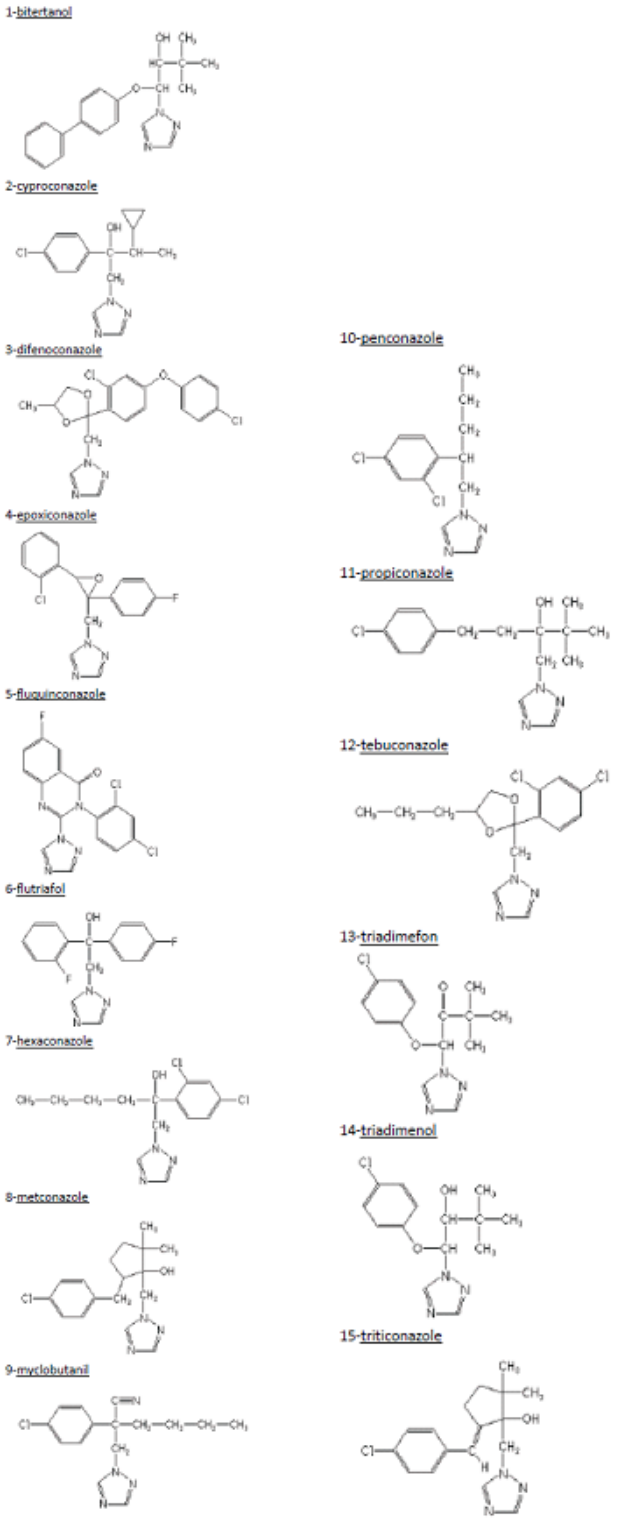

Figure 2. Human placental aromatase cytochrome P450 aromatase (CYP19A1) refined at 2.75 angstrom 3S79 (ribbon model). Source: http://www.rcsb.org/pdb/explore/jmol.do?structureId=3S79]

Figure 3. Target pocket surrounding Heme-molecule of aromatase CYP19A1

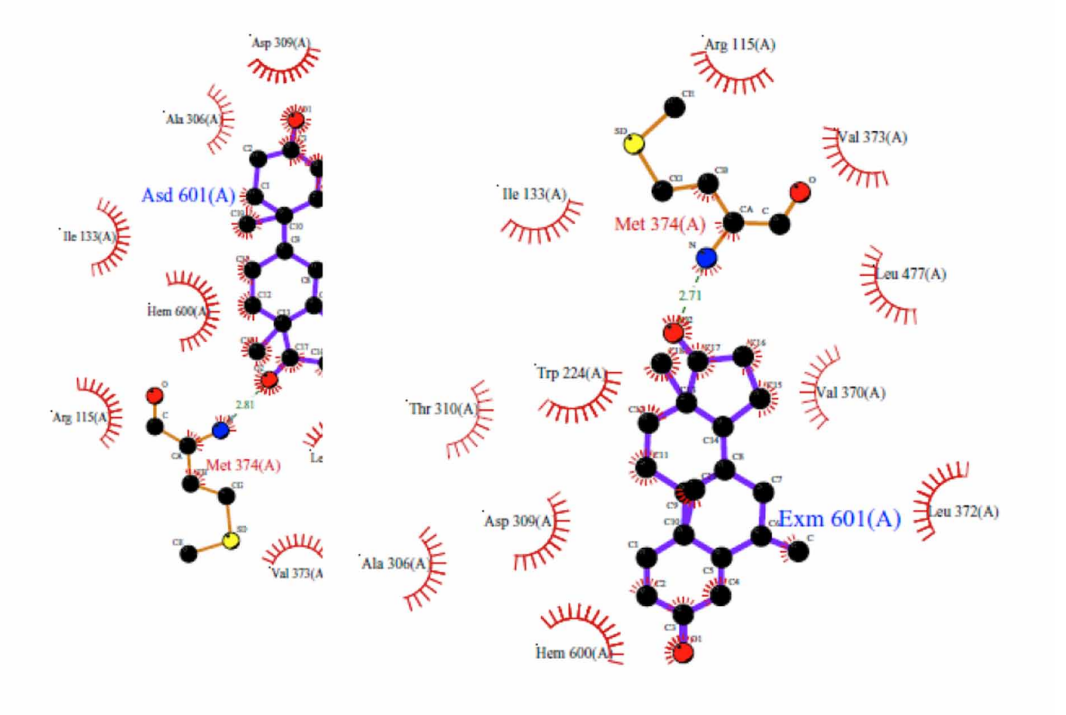

Figure 4. Compound 1 docked within the binding pocket of the enzyme 3S79.Predicted binding mode of compound 1 ().On the left, stick and ball model, and on the right, ribbon model of enzyme 3S79 in the binding pocket of which compound 1 is forming hydrogen bond with the amino acids ASP371 and LEU372

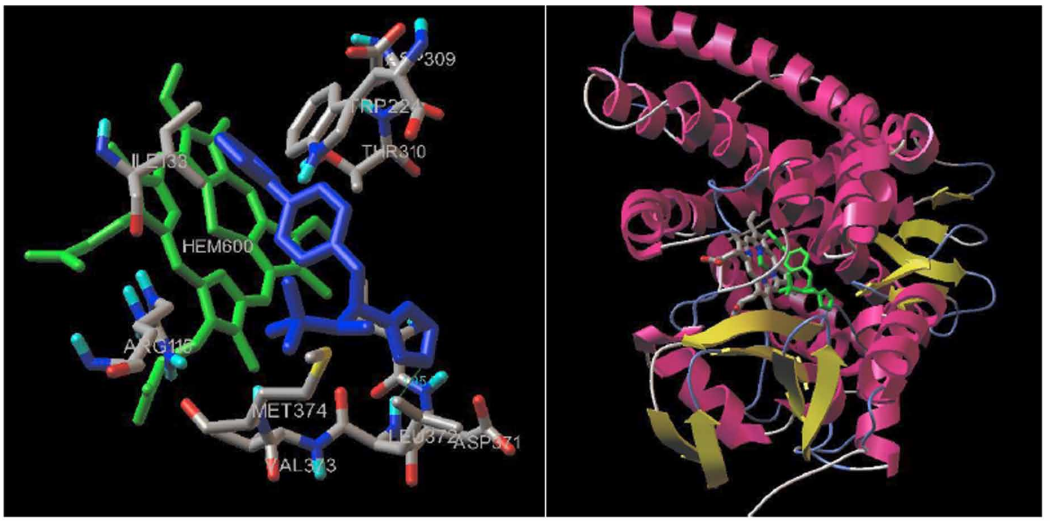

Figure 5. Predicted binding mode of compound 3.On the left, stick and ball model, and on the right, ribbon model of enzyme 3S79 in the binding pocket of which compound 3 is forming hydrogen bond with the amino acid THR310

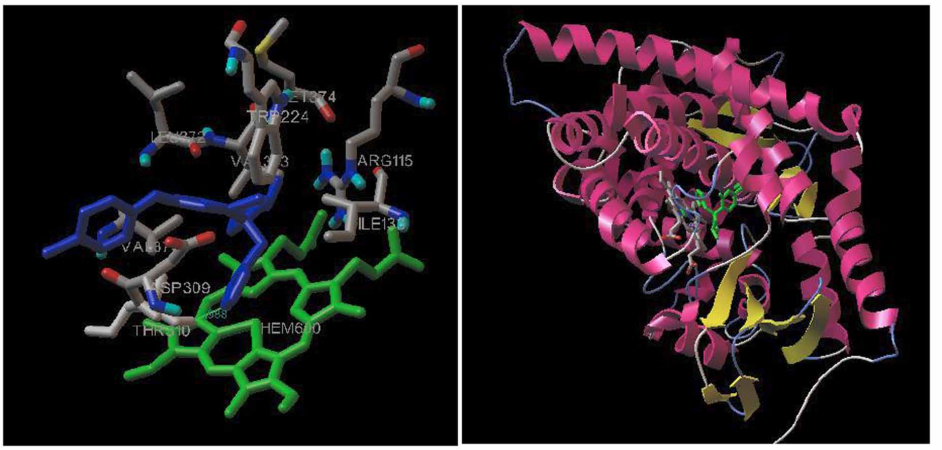

Figure 6. Predicted binding mode of compound 10.On the left, stick and ball model, and on the right, ribbon model of enzyme 3S79 in the binding pocket of which compound 3 is forming hydrogen bond with the amino acid THR310

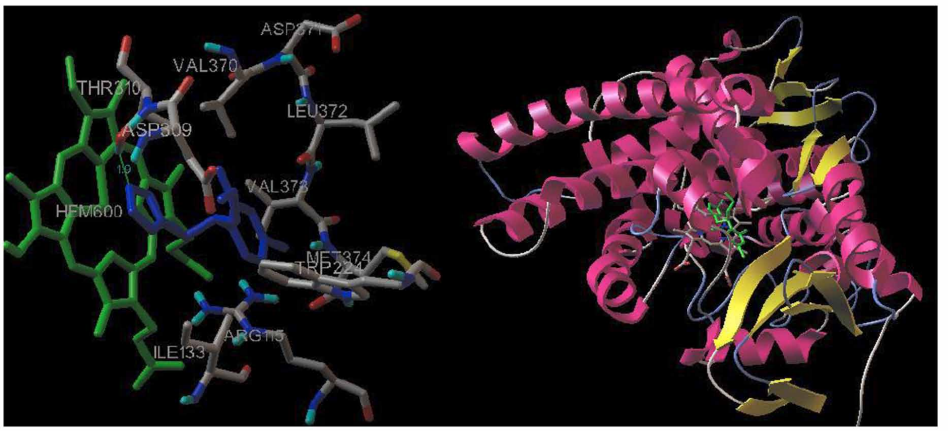

Figure 7. Reference compound, Letrozole docked in the binding pocket of the enzyme 3S79. (Ball and stick model and ribbon model)

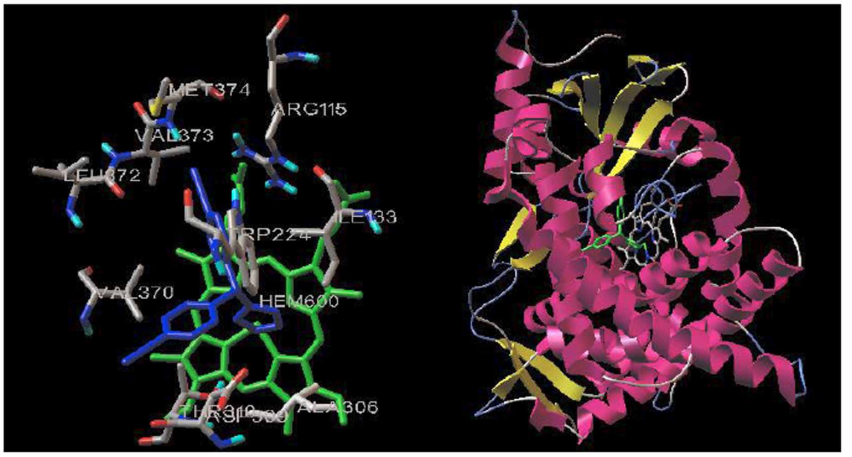

In our study we found that four triazole fungicides compounds 15, 12, 8, 5 exhibited minimal inhibition constant (IC). Those are Triticonazole, Tebuconazole, Metconazole and Fluquinconazole. (Figures 8, 9, 10, 11).

Compound 15 exhibits its binding energy -21.65 at orientation 2nd to heme molecule parallel alignment at RMS zero point, IC – 1.35X10-016 and no H-BOND.

Figure 8. Molecular surface view of compound 15 docked within the binding pocket of the enzyme 3S79 without H-bonds.Predicted binding mode of compound 15 (Triticonazole)

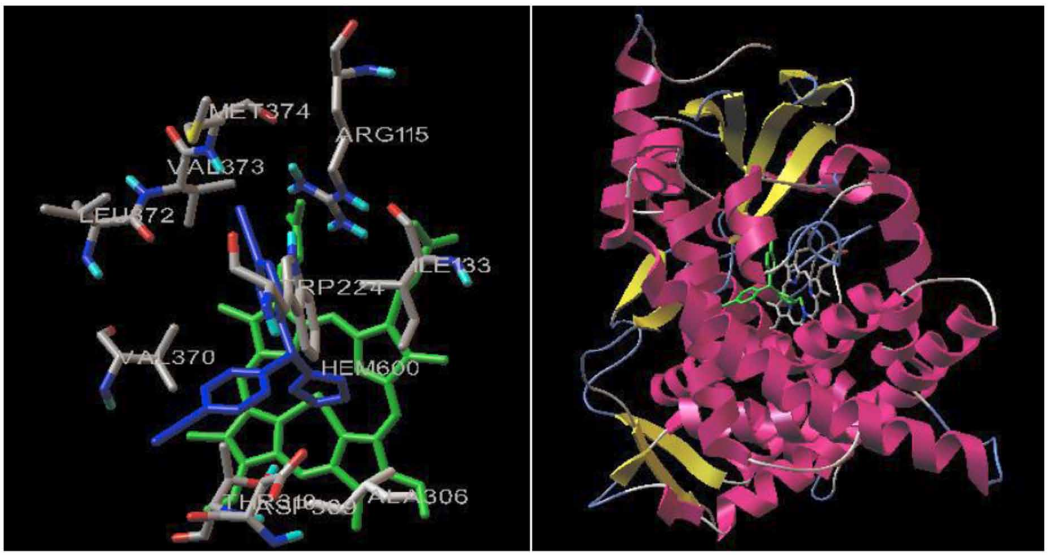

Figure 9. Molecular surface view of compound 12 docked within the binding pocket of the enzyme 3S79 without H-bonds. Predicted binding mode of compound 12 (Tebuconazole)

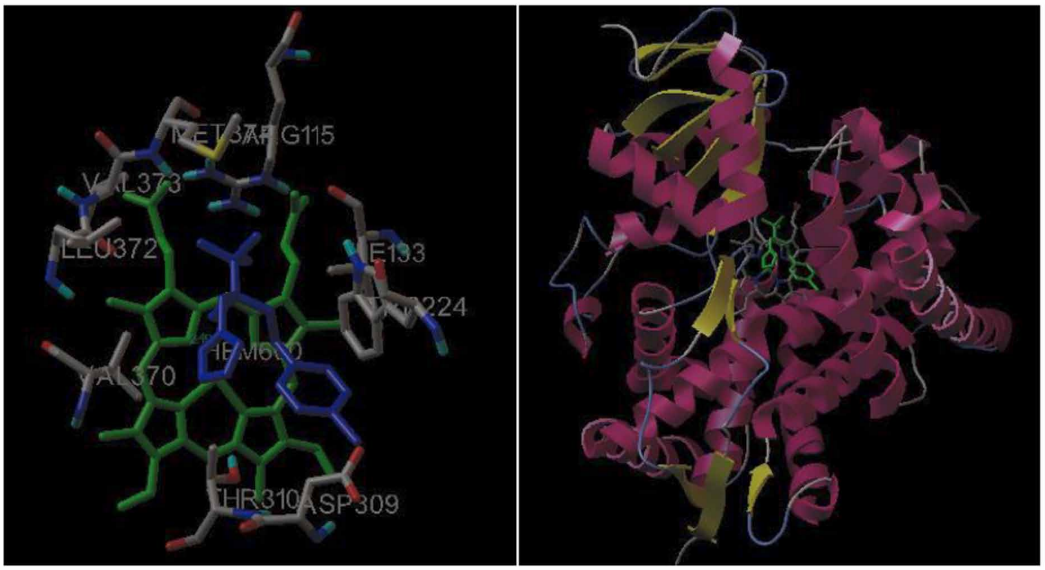

Figure 10. Molecular surface view of compound 8 docked within the binding pocket of the enzyme 3S79 without H-bonds. Predicted binding mode of compound 8 (Metconazole)

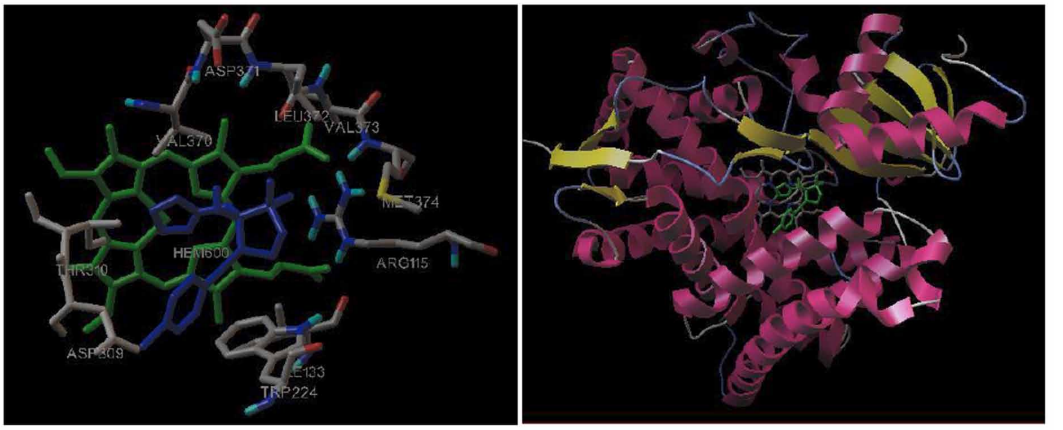

Figure 11. Molecular surface view of compound 5 docked within the binding pocket of the enzyme 3S79 without H-bonds. Predicted binding mode of compound 5 (Fluquinconazole)

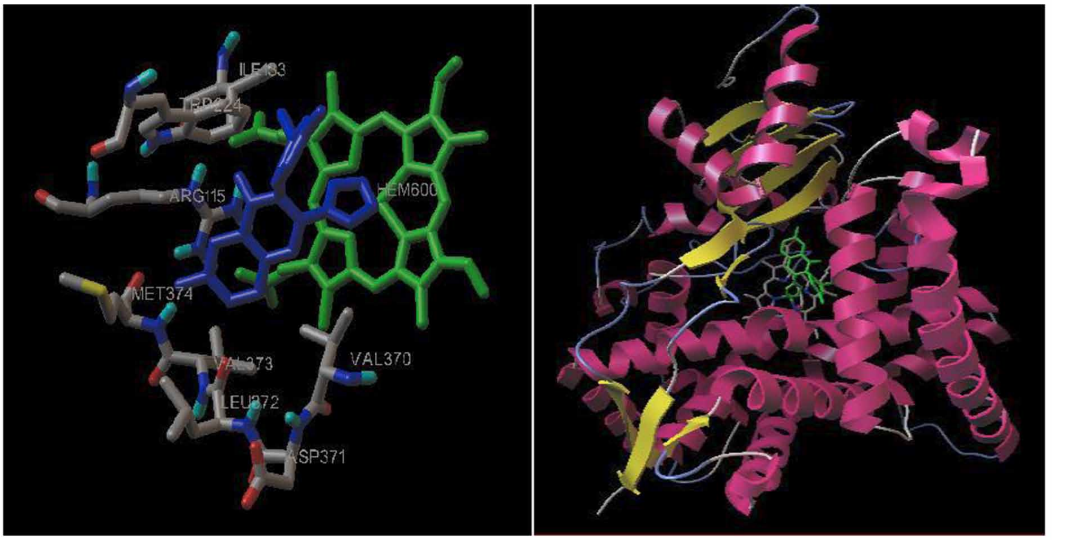

Compound 12 exhibits its binding energy -21.09 at orientation 7th to heme molecule parallel alignment at RMS zero point, IC – 3.5X 10-016 and no H-BOND.

Compound 8 exhibits its binding energy -19.69 at orientation 5th to heme molecule parallel alignment at RMS zero point, IC – 3.68X10-015 and no H-BOND.

Compund 5 exhibits its binding energy -17.25 at orientation 9th to heme molecule parallel alignment at RMS zero point, IC 2.29 X10-013 and no H-BOND.

CONCLUSION

Those compounds with minimal binding energy are safer in terms of toxicity and resistance of other prescription drugs like non-steroid AIs. Those with higher binding energies may cause drug resistance or toxicity in cases of other triazole containing drugs like Letrozole.

REFERENCES

Amarneh, B., Corbin, C., Peterson, J., Simpson, E., & Graham-Lorence, S. (1993). Functional domains of human aromatase cytochrome P450 characterized by linear alignment and site-directed mutagenesis. *Molecular Endocrinology (Baltimore, Md.)*, *7*(12), 1617–1624. PMID:8145767

Barril, X., & Morley, S. (2005). Unveiling the full potential of flexible receptor docking using multiple crystallographic structures. *Journal of Medicinal Chemistry*, *48*(13), 4432–4443. doi:10.1021/jm048972v PMID:15974595

Brodie, A. (2002). Aromatase inhibitors in breast cancer. *Trends in Endocrinology & Metabolism*, 13(2), 61-65.

Brueggemeier, R., Hackett, J., & Diaz-Cruz, E. (2005). Aromatase Inhibitors in the Treatment of Breast Cancer. *Endocrine Reviews*, *26*(3), 331–345. doi:10.1210/er.2004-0015 PMID:15814851

Chen, S., Besman, M., Sparkes, R., Zollman, S., Klisak, I., Mohandas, T., & Shively, J. et al. (1988). Human aromatase: cDNA cloning, Southern blot analysis, and assignment of the gene to chromosome 15. *DNA (Mary Ann Liebert, Inc.)*, *7*(1), 27–38. doi:10.1089/dna.1988.7.27 PMID:3390233

Chumsri, S., Howes, T., Bao, T., Sabnis, G., & Brodie, A. (2011). Aromatase, Aromatase Inhibitors, and Breast Cancer. *The Journal of Steroid Biochemistry and Molecular Biology*, *125*(1-2), 13–22. doi:10.1016/j.jsbmb.2011.02.001 PMID:21335088

Egbuta, C., Lo, J., & Ghosh, D. (2014). Mechanism of inhibition of estrogen biosynthesis by azole fungicides. *Endocrinology*, *155*(12), 4622–4628. doi:10.1210/en.2014-1561 PMID:25243857

Favia, A., Cavalli, A., Masetti, M., Carotti, A., & Recanatini, M. (2006). Three-dimensional model of the human aromatase enzyme and density functional parameterization of the iron-containing protoporphyrin IX for a molecular dynamics study of heme-cysteinato cytochromes. *Proteins*, *62*(4), 1074–1087. doi:10.1002/prot.20829 PMID:16395678

Feng, D., Guo, J., Song, W., Hu, W., & Li, Z. (2011). Comparative quantitative structure–activity relationship (QSAR) study on acute toxicity of triazole fungicides to zebrafish. *Chemistry and Ecology*, *27*(4), 359–368. doi:10.1080/02757540.2011.585780

Geisler, J. (2011). Differences between the non-steroidal aromatase inhibitors anastrozole and letrozole - of clinical importance? *British Journal of Cancer*, *104*(7), 1059–1066. doi:10.1038/bjc.2011.58 PMID:21364577

Ghosh, D., Griswold, J., Erman, M., & Pangborn, W. (2009). Structural basis for androgen specificity and oestrogen synthesis in human aromatase. *Nature*, 457(7226), 219-23.

Ghosh, D., Griswold, J., Erman, M., & Pangborn, W. (2010). X-ray structure of human aromatase reveals an androgen-specific active site. *The Journal of Steroid Biochemistry and Molecular Biology*, *118*(4-5), 197–202. doi:10.1016/j.jsbmb.2009.09.012 PMID:19808095

Ghosh, D., Lo, J., Morton, D., Valette, D., Xi, J., Griswold, J., & Davies, H. M. L. et al. (2012). Novel Aromatase Inhibitors by Structure-Guided Design. *Journal of Medicinal Chemistry*, *55*(19), 8464–8476. doi:10.1021/jm300930n PMID:22951074

Jeannot, R., Sabik, H., Sauvard, E., & Genin, E. (2000). Application of liquid chromatography with mass spectrometry combined with photodiode array detection and tandem mass spectrometry for monitoring pesticides in surface waters. *Journal of Chromatography. A*, *879*(1), 51–71. doi:10.1016/S0021-9673(00)00098-4 PMID:10870695

Karkola, S., Holtje, H., & Wahala, K. (2007). A three-dimensional model of CYP19 aromatase for structure-based drug design. *Steroid Biochem. Mol. Biol.*, *105*(1-5), 63–70. doi:10.1016/j.jsbmb.2006.11.023 PMID:17583493

Kumar, V., Ravindranath, S., & Shanker, A. (2004). Fate of hexaconazole residues in tea and its behavior during brewing process. *Journal of Chemical Health and Safety*, *11*(1), 21–25. doi:10.1016/j.chs.2003.09.018

Morris, G., Goodsell, D., Halliday, R., Huey, R., Hart, W., Belew, R., & Olson, A. (1998). Automated docking using a Lamarckian genetic algorithm and empirical binding free energy function. *Journal of Computational Chemistry*, *19*(14), 1639–1662. doi:10.1002/(SICI)1096-987X(19981115)19:14<1639::AID-JCC10>3.0.CO;2-B

Morris, G., Goodsell, D., Halliday, R., Huey, R., Hart, W., Belew, R., & Olson, A. (1998). Automated docking using a Lamarckian genetic algorithm and an empirical binding free energy function. *Journal of Computational Chemistry*, *19*(14), 1639–1662. doi:10.1002/(SICI)1096-987X(19981115)19:14<1639::AID-JCC10>3.0.CO;2-B

Paraíba, L. (2007). Pesticide bioconcentration modelling for fruit trees. *Chemosphere*, *66*(8), 1468–1475. doi:10.1016/j.chemosphere.2006.09.017 PMID:17092536

Schuster, D., Laggner, C., Steindl, T., Palusczak, A., Hartmann, R., & Langer, T. (2006). Pharmacophore modeling and in silico screening for new P450 19 (aromatase) inhibitors. *Journal of Chemical Information and Modeling*, *46*(3), 1301–1311. doi:10.1021/ci050237k PMID:16711749

Singer, H. (2002). Pesticides in Water - Research Meets Politics. *J. EAWAG News*, *59*, 16–19. http://www.swissinfo.ch/eng/pollution_pesticide--cocktail--found-in-swiss-rivers/38096166

Snelders, E., Camps, S., Karawajczyk, A., Schaftenaar, G., & Kema, G. et al.. (2012). *Triazole Fungicides Can Induce Cross-Resistance to Medical Triazoles in Aspergillus fumigatus*. J. PLOS ONE. Doi: doi:10.1371/journal.pone.0031801

Solis, F., & Wets, R. (1981). Minimization by random search techniques. *Mathematics of Operations Research*, *6*(1), 19–30. doi:10.1287/moor.6.1.19

Suvannang, N., Nantasenamat, C., Isarankura-Na-Ayudhya, C., & Prachayasittikul, V. (2011). Molecular docking of Aromatase Inhibitors. *Molecules (Basel, Switzerland)*, *16*(5), 3597–3617. doi:10.3390/molecules16053597

Thompson, E., Jr., & Siiteri, P. (1974). Utilization of oxygen and reduced nicotinamide adenine dinucleotide phosphate by human placental microsomes during aromatization of androstenedione. *J. Biol. Chem*., 249(17), 5364-5372.

Trösken, E., Bittner, N., & Völkel, W. (2005). Quantitation of 13 azole fungicides in wine samples by liquid chromatography–tandem mass spectrometry. *Journal of Chromatography. A*, *1083*(1-2), 113–119. doi:10.1016/j.chroma.2005.06.020 PMID:16078696

Zarn, J., Brüschweiler, B., & Schlatter, J. (2003) Azole Fungicides Affect Mammalian Steroidogenesis by Inhibiting Sterol 14α-Demethylase and Aromatase. *Environmental Health Perspectives,* 111(3), 255–261.

Zhou, Q., Xiao, J., & Ding, Y. (2007). Sensitive determination of fungicides and prometryn in environmental water samples using multiwalled carbon nanotubes solid-phase extraction cartridge. *Analytica Chimica Acta*, *602*(2), 223–228. doi:10.1016/j.aca.2007.09.038 PMID:17933607